

The Variable X-ray Sky as Seen by Chandra:

- Among the variable sources observed by Chandra are stars; compact objects (white dwarfs, neutron stars, black holes) within our own Galaxy, and in other galaxies; Active Galactic Nuclei, etc.
- Variable behavior can include random, aperiodic variability; transient phenomena such as flares; periodic variability, such as orbital modulation and eclipses, etc.
- Variability can occur within an observation, and/or between multiple observations of the same object.

Chandra Time Scales:

- Integration (frame) times can range from 0.2-3.2 seconds for ACIS, which yield the fastest time scales discernible within the current catalog. (Continuous clocking mode observations, not included in the catalog, cover msec time scales. HRC also allows fast timing capability, but limited spectral resolution.)
- Individual observation lengths range from ≈ 1 ksec-160 ksec.
- Multiple observations of the same fields and sources can span time scales ranging from days to years.
- Variable sources on all of these time scales can be found within the catalog.

Challenges of Discerning Variability with Chandra Observations:

- The Chandra spacecraft pointing position dithers in a *lissajous pattern* with periods of 707 and 1000 seconds (for the ACIS detector).
- This dither pattern can carry source regions over chip edge boundaries, across bad pixels and bad columns, across CCD node boundaries, etc.
- The background can vary over the course of an observation. Although this is not a serious issue for point sources near the optical axis, it can be more significant for extended sources, or sources far off-axis.
- The same source viewed across multiple observations may have had very different instrumental configurations, e.g., backside-illuminated vs. frontside-illuminated CCD, on-axis vs. far off-axis, etc.

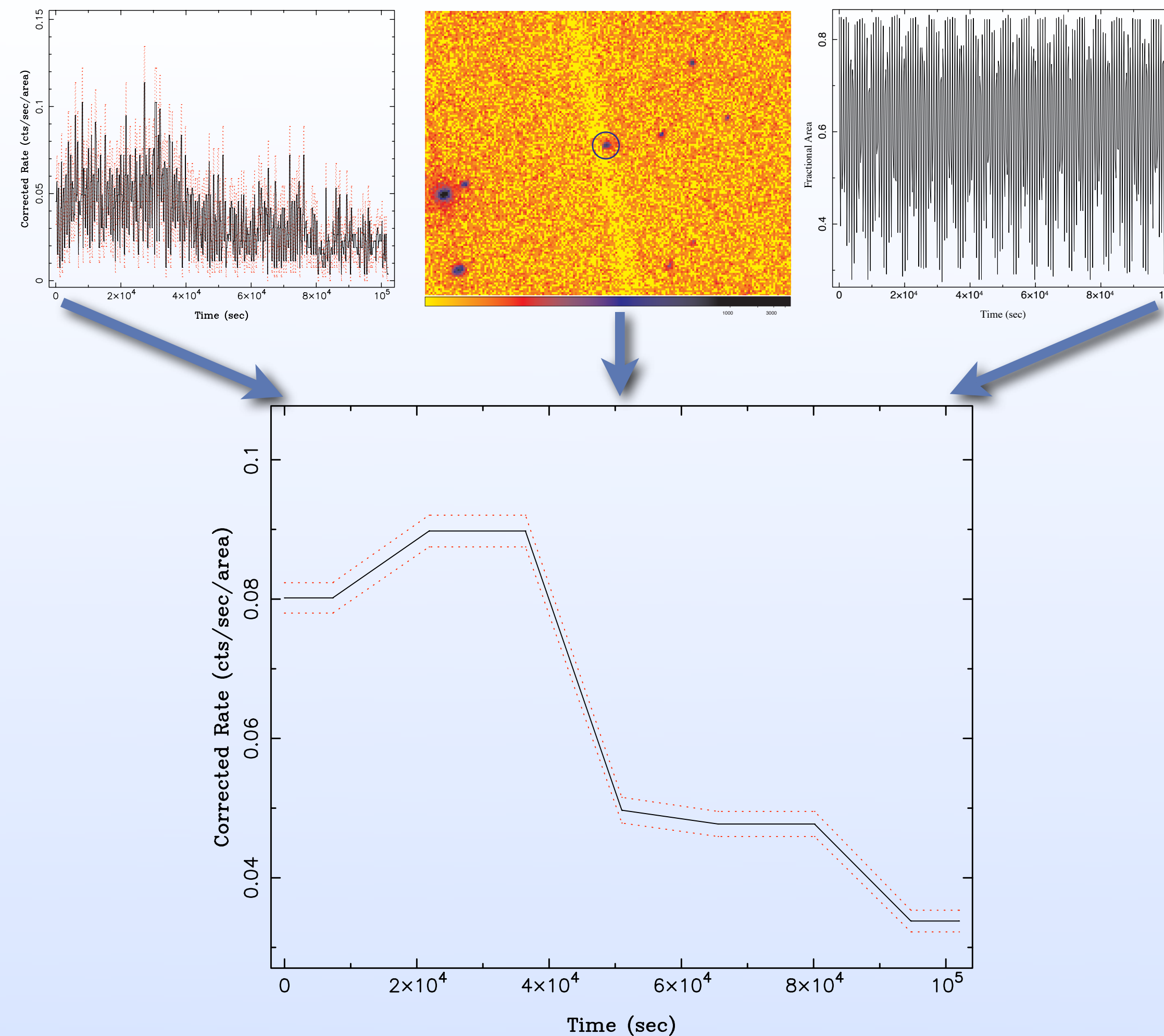


Figure 1: Sources can overlap chip boundaries (top middle), and/or dither over bad pixels and columns. This leads to an instrumental modulation of the count rate (top left). The *dither_region* tool is applied to all catalog sources, and a geometric fractional area correction (top right) is applied to all lightcurves in the computation of all variability tests. The best estimate lightcurves have these geometric effects removed (bottom).

Lightcurve Preparation Procedures:

- Excise times of high background. A compromise is chosen between reducing signal-to-noise for on-axis point sources, and increasing signal-to-noise for extended or off-axis sources.
- The tool *dither_region* is applied, which calculates the time-dependent normalized geometric region, accounting for bad pixels & columns, and chip edges. It *does not account for response variations*, e.g., as a source crosses CCD nodes. Geometric corrections alone, however, reduce false positives.
- Lightcurves from a background region are also extracted.

Variability Tests:

- Three variability tests are run: Kolmogorov-Smirnov, Kuiper, and Gregory-Loredo (a Bayesian test).
- Kolmogorov-Smirnov & Kuiper tests compare the cumulative distribution of event arrival times to that expected from a constant rate. It answers: "Does my source vary?"
- Gregory-Loredo compares the likelihood that multiple, uniform time bins describe the lightcurve better than a single, constant rate bin. It answers: "Is my source described by an evenly binned lightcurve with multiple bins?"

Variability Products:

- Probability values, p , for whether the lightcurves are variable ($ks/kp/var_prob_*$) are provided for each of the three tests in each of five energy bands: ultra-soft, medium, hard, broad. ($P=1-p$ is the probability that the source is consistent with constant.)
- A lightcurve is produced based upon the results of the Gregory-Loredo analysis. This is not simply a binned lightcurve, but rather is a weighted average created using the likelihoods of each uniform binning tested. The lightcurve is stored at a resolution $3\times$ finer than the single uniform binning with the greatest likelihood.
- A variability index for each energy band is assigned to the source, based on the Gregory-Loredo test and lightcurve properties.
- Flags are set if the source dithers over a chip edge (*edge_code*), or across multiple chips (*multi_chip_code*), or if the variability is on a dither time scale (*dither_warning_flag*).

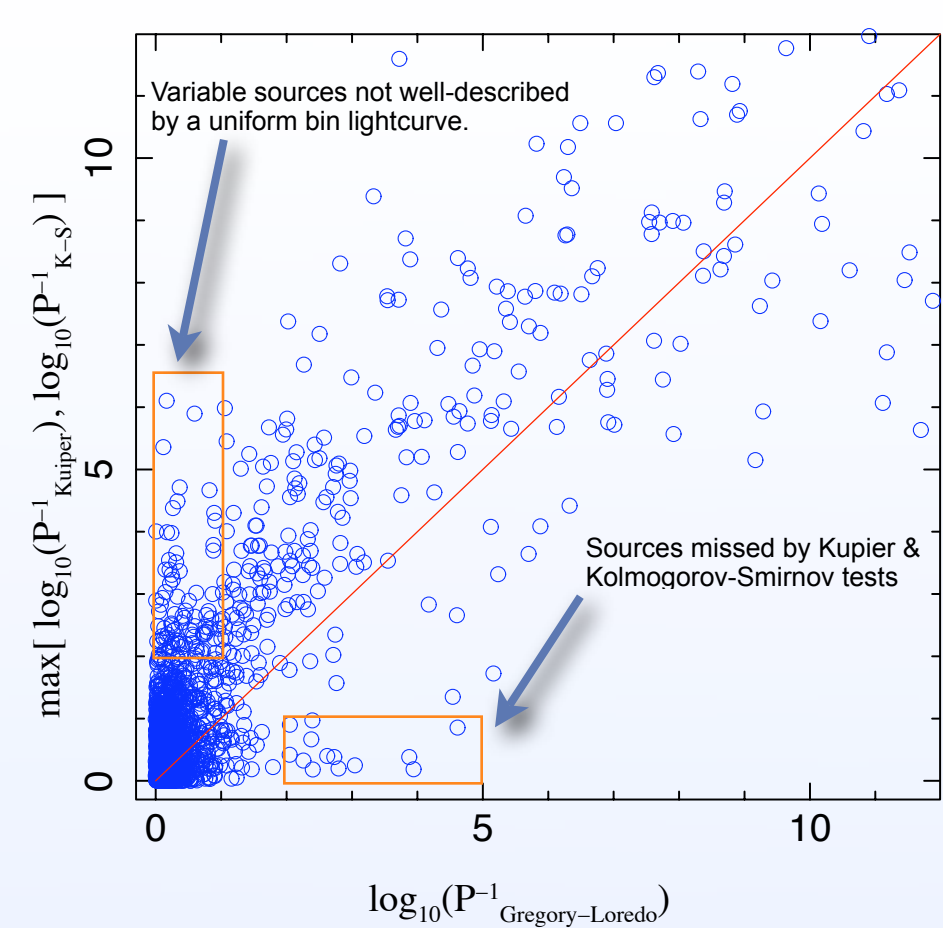


Figure 2: Comparison between catalog probability values (low P =highly variable) derived from the Gregory-Loredo test and the Kuiper and Kolmogorov-Smirnov tests. The latter two indicate more highly significant variability; however, the former also provides an estimate of the lightcurve shape (Fig. 1).

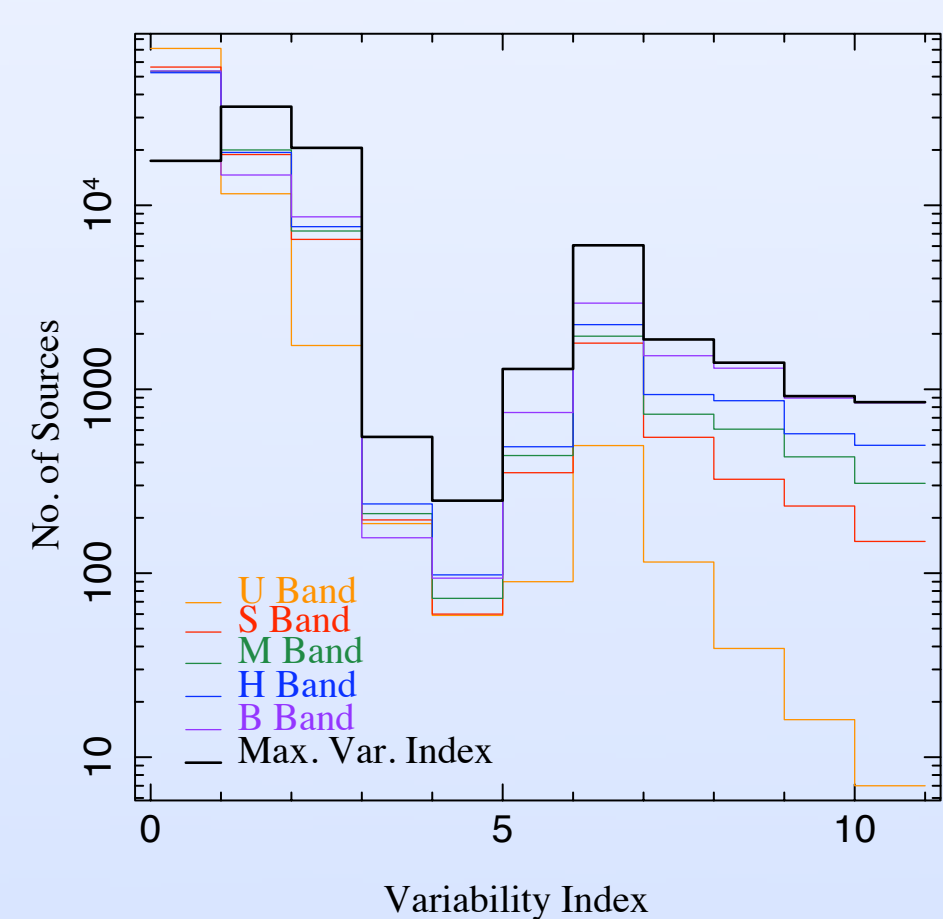


Figure 3: Distributions of variability indices for each energy band, obtained from a snapshot of the preliminary catalog results (12/19/2008). Note the bimodal distributions, and that variability is detected easiest at higher energies. Highly significant detections (max index ≥ 6) occur for 12% of sources.

Variability Index	Condition	Comment
0	$0 < p < 0.5$	No Detectable Variability
1	$0.5 < p < 0.67, f_3 > 0.997, f_5 = 1.0$	Not Likely Variable
2	$0.67 < p < 0.9, f_3 > 0.997, f_5 = 1.0$	Not Likely Variable
3	$0.5 < p < 0.6$	Possibly Variable
4	$0.6 < p < 0.67$	Possibly Variable
5	$0.67 < p < 0.9$	Likely Variable
6	$0.9 < p$ and $O < 2.0$	Very Likely Variable
7	$2 < O < 4$	Extremely Likely Variable
8	$4 < O < 10$	Variable
9	$10 < O < 30$	Variable
10	$30 < O$	Variable

Table 1: The variability index, calculated for each energy band, runs from 0-10. Here p is the probability that the lightcurve is *not* consistent with a constant rate. f_3 and f_5 are the fractions of the Gregory-Loredo generated lightcurve that lie within 3σ and 5σ of the mean value. O is the \log_{10} of the odds ratio that a multiple, uniform bin (i.e., variable) lightcurve is a better description than a single bin, constant rate lightcurve. I.e., $O = \log_{10}(P^{-1})$, where $P=1-p$ is the probability of a lightcurve consistent with constant. O is the x-axis for many of the plots shown here.

Note: For the results shown on the left and the right, only sources that did not span more than one chip and that were not dithered over a chip edge (*multi_chip_code*=0 and *edge_code*=0) were included in the figures.

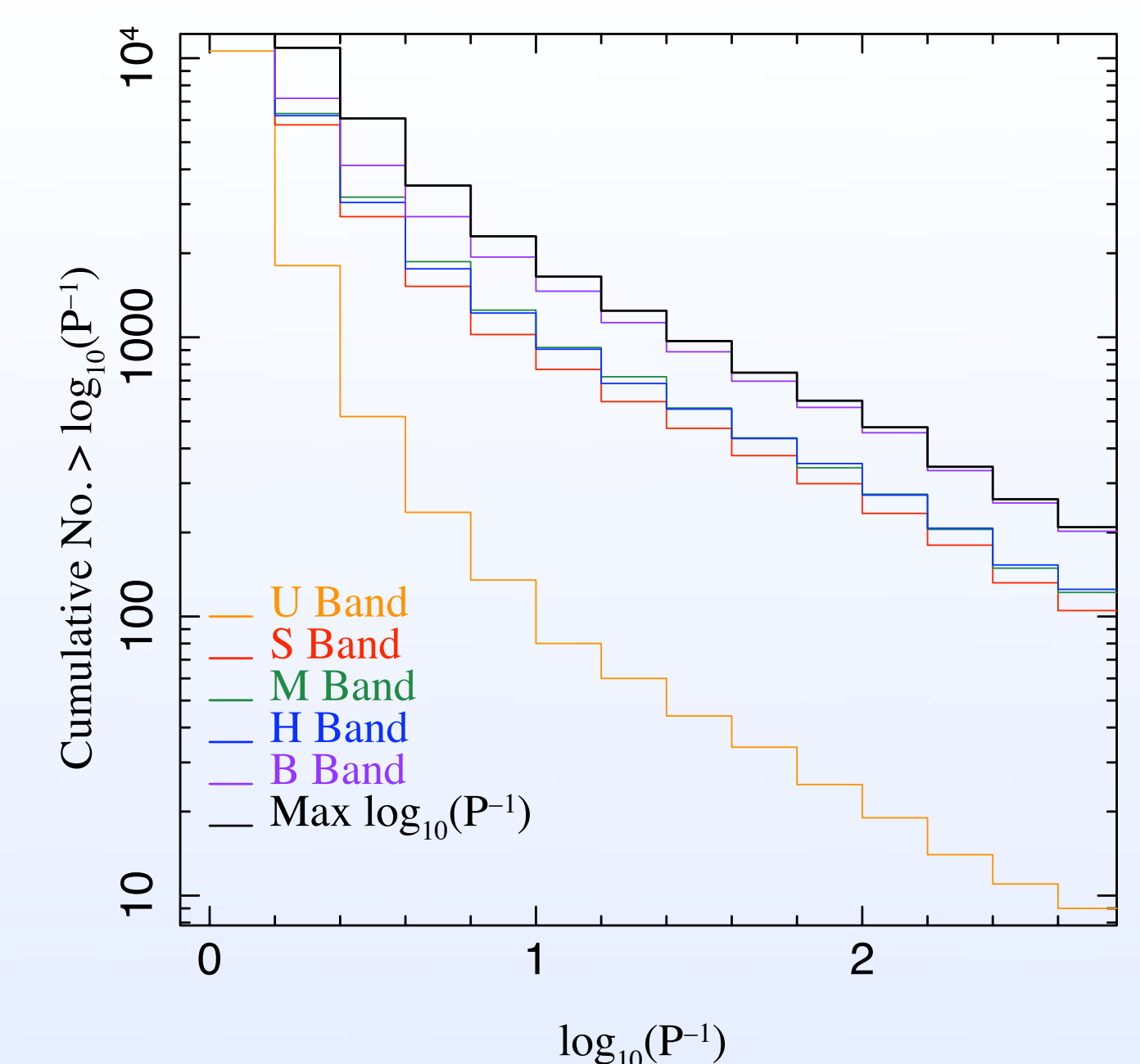


Figure 4: Of the over 17,000 unique master sources with multiple observations (Dec. 29, 2008 snapshot), nearly 500 exhibit inter-observation variability with $>99\%$ significance, primarily in the broad-band, although significant variability is seen in all bands.

Inter-Observation Variability:

- Compute fluxes and flux errors in each energy band for each observation comprising a master source, and calculate the error weighted mean fluxes.
- Tabulate the most significant (as measured in units of σ) difference between an individual observation flux and the error weighted mean flux (*var_inter_sigma*).
- Calculate the probability that the individual fluxes are consistent with a χ^2 distribution, and based upon this, assign a probability p that the source is variable (*var_inter_prob_**). ($P=1-p$ is the probability that the source is consistent with constant, and is related to the \log_{10} odds ratio by $O = \log_{10}(P^{-1})$.)

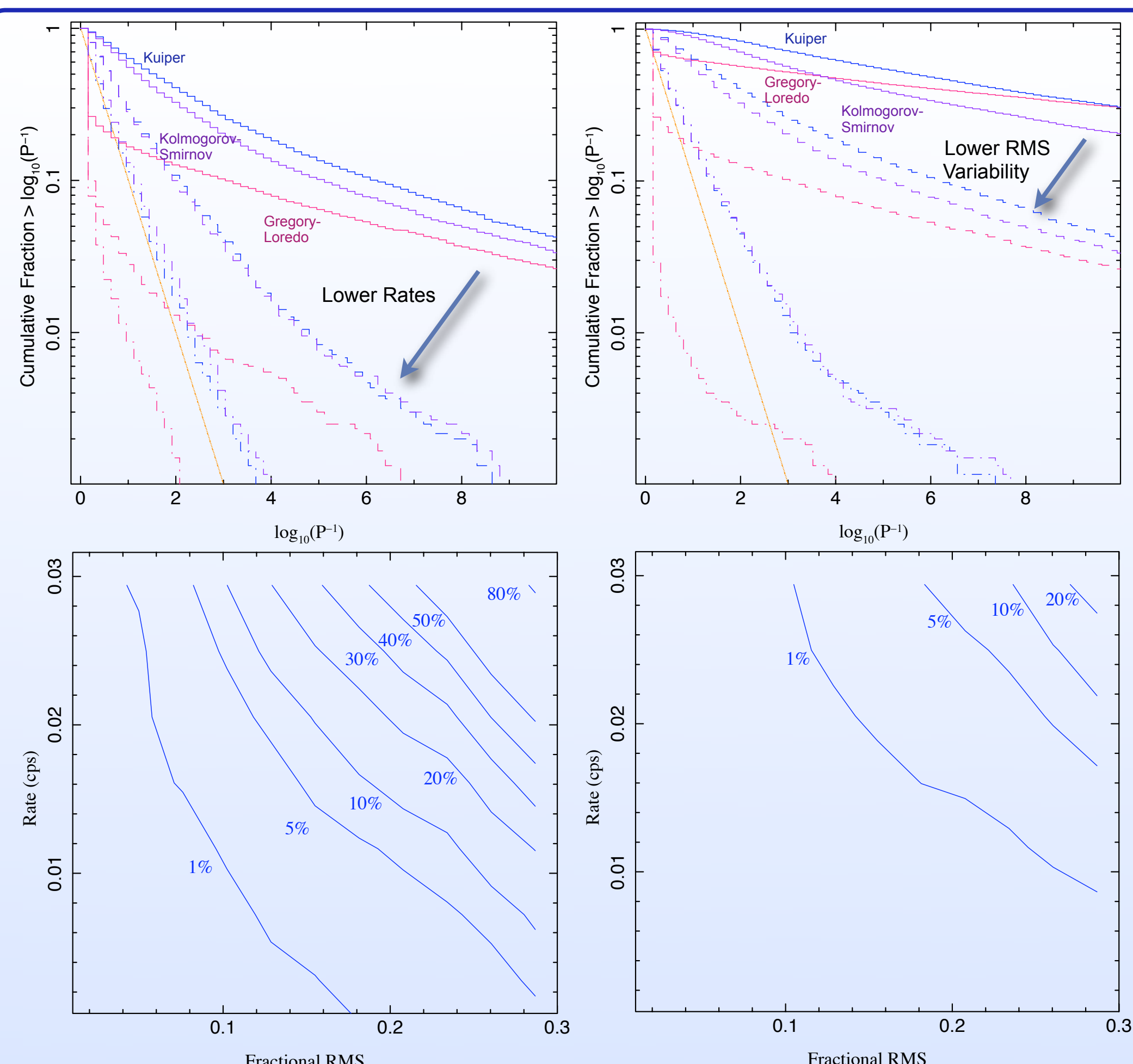


Figure 5: Top left: The cumulative fraction of simulations $>$ than a given $\log_{10}(P^{-1})$ (low P =highly variable) for the three variability tests, given 160 ksec lightcurves and a 0.15 fractional RMS variability. Rates are 0.032, 0.0056, and 0.001 cps. Top right: The fraction of simulations $>$ than $\log_{10}(P^{-1})$ for 160 ksec lightcurves and a 0.032 cps rate with RMS fractions of 0.3, 0.14, and 0.05. Bottom: Using the Kuiper test, the total fraction of simulations with $\log_{10}(P^{-1}) > 2$ as a function of fractional RMS variability and mean count rate for 160 ksec lightcurves (left) and 20 ksec lightcurves (right). I.e., these are proxies for sensitivity of the Kuiper test.

Characterization of the Variability Tests:

- A *S-lang* script was written to take an arbitrary functional form for a power spectral density (PSD), normalize it to a given fractional root mean square (RMS) amplitude, draw $\chi^2_{\nu=2}$ deviates based upon these Fourier amplitudes, and uniformly randomize the Fourier phases. These Fourier series were then inverted to yield a time domain rate.
- The time series rate was then used to draw Poisson variables in each time bin. A simple pile-up model was applied to each time bin. Each event was presumed to have a 95% chance of falling into the central, piled region. It was further assumed that for N such events, there was a probability, $\alpha^{(N-1)}$ with $\alpha=0.5$, that they would be detected as a *single* event. (Otherwise N was set to 0.)
- Lightcurves were simulated using time bins of 3.24104 sec, total lengths ranging from 1 ksec-160 ksec, and mean count rates from 5.6×10^{-4} -0.032 counts/sec.
- Lightcurves were simulated for pure white noise (i.e., constant rates, Poisson noise only), red noise ($PSD \propto f^{-1}$), and periodic signals (100 sec, 300 sec, and 1000 sec periods). Here we show red noise simulations for different RMS levels.
- The three variability tests, Kolmogorov-Smirnov, Kuiper, and Gregory-Loredo were applied to the simulations. Result highlights are shown in Fig. 5.
- White noise simulations indicate that the traditional P value is a very good indication of the significance level of the Kolmogorov-Smirnov and Kuiper tests, even when including pile-up.
- The Gregory-Loredo test tends to give "less significant" (i.e., larger) P values, but it is asking a more restrictive question - not "Does my source vary?", rather "Is my source described by an evenly binned lightcurve with multiple bins?"
- Point source simulations with *MARX* (see Posters 472.05 & 472.06) essentially create white noise (constant rate) lightcurves, and are passed through the Chandra Catalog Pipeline (see Poster 472.07), including variability tests. These simulations therefore become indicators of false variability detection. Variability results from these simulations are presented in Fig. 6.

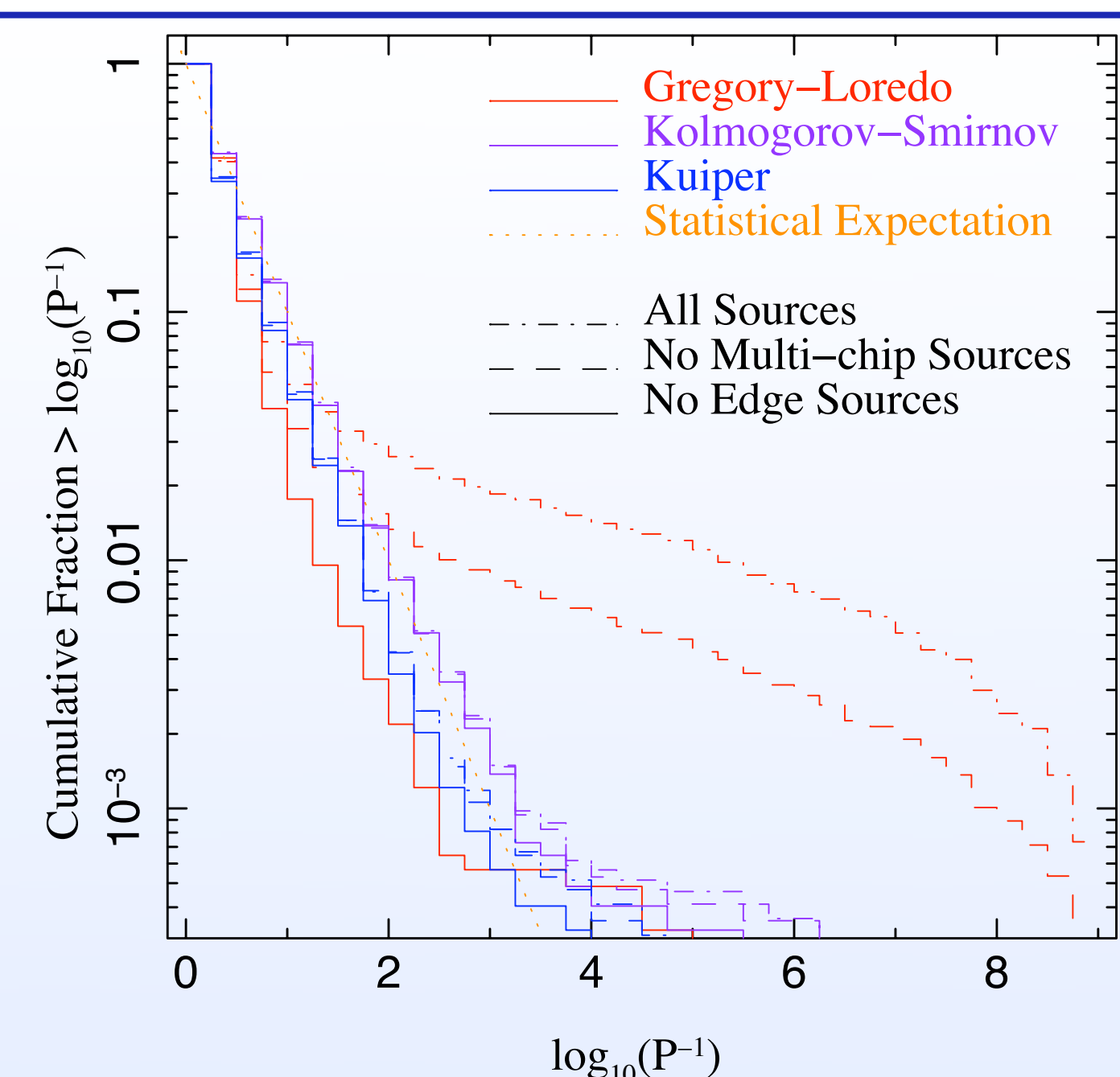


Figure 6: Variability results for simulated constant rate, power-law spectra sources (see Poster 472.07). Over 19,000 sources pass the catalog inclusion criteria, and of these, over 12,000 do not span more than one chip, nor have regions that overlap a chip edge. These latter sources agree well with statistical expectations, and have "false variability rates" (i.e., cumulative fractions exceeding the statistical expectations) of $<0.1\%$. For sources that span multiple chips, or overlap chip edges, the false variability rate is higher, especially for the Gregory-Loredo test. For that test, however, the application of the *dither_region* tool correction is only approximate (i.e., there are implicit assumptions made by the Gregory-Loredo algorithm that can be violated in reality, as opposed to the geometrical area correction in the Kolmogorov-Smirnov and Kuiper tests, where the application is exact). For a variety of reasons, we consider the above results as "upper limits" to the false variability rate, and we will further refine these estimates during the catalog characterization process.

Acknowledgements:

This work was supported by NASA Contracts NAS8-03060 and SV3-73016.